International Journal of Impact Engineering 37 (2010) 317–323

Contents lists available at ScienceDirect

International Journal of Impact Engineering

journal homepage: www.elsevier.com/locate/ijimpeng

An active concept for limiting injuries caused by air blasts

H.N.G. Wadley [a], K.P. Dharmasena [a,*], M.Y. He [b], R.M. McMeeking [b], A.G. Evans [b], T. Bui-Thanh [c], R. Radovitzky [c]

[a] Department of Materials Science & Engineering, University of Virginia, Charlottesville, VA 22904, USA
[b] Departments of Materials and Mechanical Engineering, University of California at Santa Barbara, Santa Barbara, CA 93106, USA
[c] Department of Aeronautics and Astronautics, Massachusetts Institute of Technology, Cambridge, MA 02139, USA

ARTICLE INFO

Article history:
Received 29 July 2008
Received in revised form
6 January 2009
Accepted 12 June 2009
Available online 21 June 2009

Keywords:
Air blasts
Active mitigation
Cellular materials
Deployable structures
Reactive armor

ABSTRACT

We explore the feasibility of cellular materials concepts for passive and active mitigation of blast overpressures. The passive approach requires a cellular medium that compresses at nominally constant stress and dissipates the kinetic energy acquired by an attached buffer plate. Provided the cellular material is not compressed beyond its densification strain, the transmitted pressure is approximately the dynamic crush strength of the medium. This can be set just below a damage threshold by appropriate selection of the cellular material, its topology and relative density. However, for many realistic blast scenarios, the thicknesses required to avoid excess densification are excessive. The alternative is a deployable, precompressed, cellular medium released just prior to the arrival of the blast-created impulse. This accelerates an attached buffer toward the blast and creates momentum opposing that acquired from the blast. Numerical simulations of the fully coupled fluid structure interaction in air show that momentum cancellation is feasible, enabling a protective structure having much smaller volume.

1. Introduction

Explosions in air create intense shock waves capable of transferring large transient pressures and impulses to the objects they intercept [1–3]. The traveling shock comprises a strong positive pulse followed by a weaker rarefaction, Fig. 1. The peak overpressure, p_o, scales as: $p_o \sim m_{exp}/R^3$, with m_{exp} the mass of the explosive and R the distance from the explosion. The pressure-time integral represents the impulse per unit area, I, carried by the shock. The incident wave front is partially reflected at a surface [1–6] amplifying the disturbance that enters a structure. Upon entering a body, the differential displacements set-up in tissues of differing compliance and density can cause tearing of muscle tissue, blood vessels and neurons [7–14]. Studies using animal models exposed to explosions have revealed that both the pressure and duration of the shock affect the probability of injury [15–17]. For detonations of high explosives (with decay time ~0.1–1 ms), a peak overpressure of 0.3 MPa (three atmospheres) can cause injury to the thorax, while a peak pressure of 1 MPa usually results in death. *For the present assessment, we will require that each mitigation concept assures that the transmitted pressure behind a mitigation system never exceeds a threshold,* $p_{th} \approx 0.3$ MPa.

A passive strategy for mitigation entails the use of perforated plates [18], cellular media [19,20] such as polymer, metal or ceramic (pumice granules) foams, and various unconsolidated ballistic fabrics. It will be shown that, for representative loadings, significant mitigation can only be achieved by using excessively bulky or heavy buffer plate systems. For air blasts, these limitations can be overcome through active mitigation concepts in which a cellular material is compressed and then deployed just prior to arrival of the shock disturbance. The key feature of such an active (deployable) strategy is momentum cancellation. Other examples of active concepts can be found the helicopter industry [21], hydraulic actuator based active impact control (or absorption) [22], and sensor-based pedestrian protection systems [23,24]. A deployable concept based on momentum cancellation utilizing a precompressed cellular core sandwich panel is proposed and evaluated by simulations with varying levels of fidelity. To define and support the concept, the basic characteristics of air shocks, and their interactions with static structures, are first summarized. Thereafter, the interactions with moving plates are analyzed and used to chart the velocities of deployable buffers.

2. Impulses, pressures and arrival times

The free-field pressure–time response from an explosion in air is described by,

* Corresponding author.
E-mail address: kumar@virginia.edu (K.P. Dharmasena).

0734-743X/$ – see front matter © 2009 Published by Elsevier Ltd.
doi:10.1016/j.ijimpeng.2009.06.006

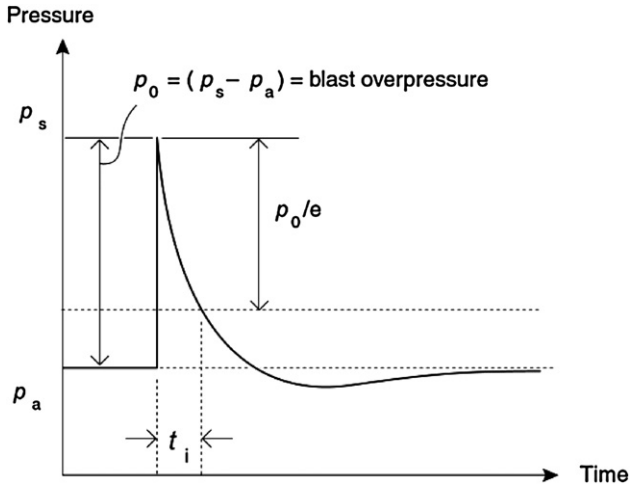

Fig. 1. The temporal variation of the pressure as an explosively created air shock propagates through a measurement point. The initial compressive phase is followed by a weak rarefaction.

$$p(x,t) = p_0 e^{(x-a_0 t)/a_0 t_i} \quad (1)$$

where $p(x,t)$ is the pressure at a point x and time t, p_o is the maximum incident overpressure, t_i is the wave decay time and a_0 is the sound speed in air. In this simplified description, the wave propagates to the right within the domain $x \leq 0$ without changing its shape and reaches the plate at time, $t = 0$. When the (compressed) shock encounters a surface, it is reflected, amplifying the overpressure. For weak shocks in air, the reflection is linear and the reflection coefficient is 2. However, the magnification can be highly non-linear and depends upon the degree of compression of the incident shock and the constitutive response of air. For strong shocks in ideal gases, the theoretical limit for the reflection coefficient is 8. However, values up to 20 have been reported when real gas effects such as the dissociation and ionization of air molecules are considered [1]. Exact calculations of the fluid–structure interaction and the pressures and impulses transferred to the structure require sophisticated coupled Euler–Lagrangian computations. Reasonable estimates can be made for the air blast loading of a rigid plate from empirical expressions developed for freely propagating shocks created by explosions [4], or by software incorporating these relations, such as the ConWep code [6]. For a known explosive material, charge mass and standoff, the code allows determination of the incident and reflected pressures and impulses, as well as the arrival time of the blast wave. It assumes that the interaction of the blast wave with a structure is decoupled. Coupled fluid-structure interaction effects on the air-blast loading are described elsewhere [25–30].

In the ensuing study, potential mitigation strategies are assessed for a model problem consisting of 10 kg of a high explosion (TNT) at a 1–10 m standoff. The relevant ConWep computations of peak pressure, impulse and arrival time as a function of range are plotted in Fig. 2.

3. The passive concept

The use of cellular materials for mitigation is conceptually straightforward. Between the blast and the structure to be protected, an intervening medium is used that reduces the pressure from $p_0 \rightarrow p_{th}$. This medium must be capable of large volume

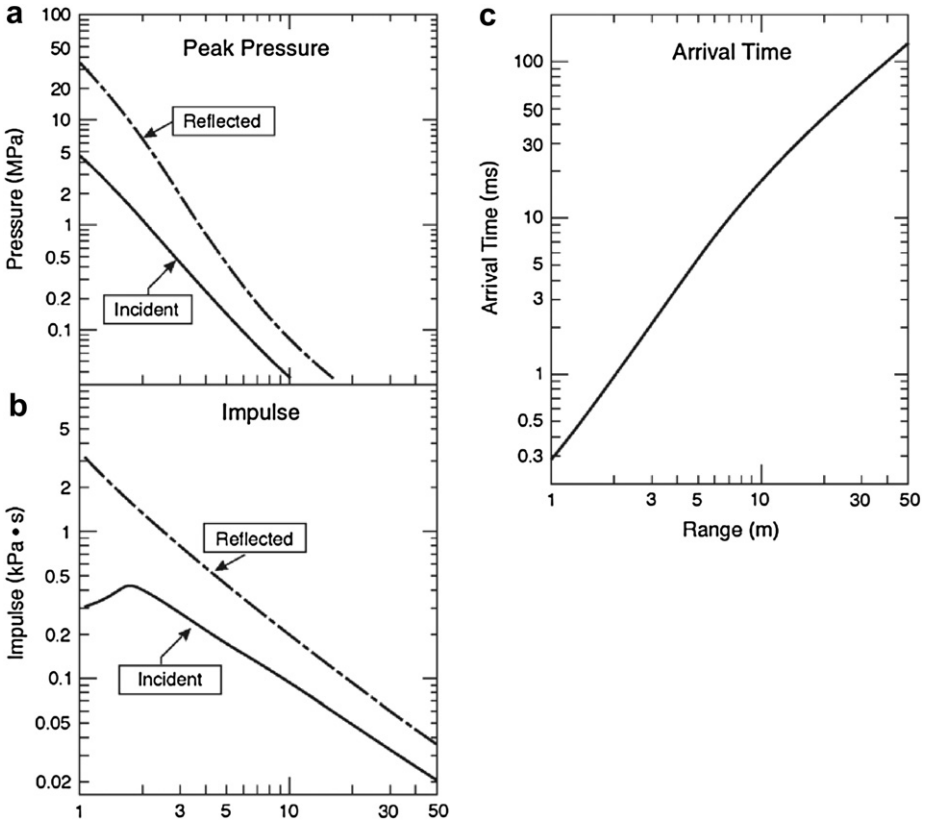

Fig. 2. ConWep calculations of the pressure and impulse when a blast due to a 10 kg TNT explosion reflects from a rigid surface: (a) the incident and reflected pressure, (b) the incident and reflected impulse. (c) The time of arrival of the shock as a function of distance from the source.

decrease at essentially constant pressure (Fig. 3). Solids and fluids are not suitable because they are incompressible. The only materials having the appropriate characteristic are low density cellular solids such as reticulated polymers, metal foams [19,20], partially pre-crushed honeycombs [31] and certain lattice solids [32] with low relative density, $\overline{\rho}$ (in the 1–10% range, i.e. with pore volume fractions of 90–99%). Examples of the topologies of some of the many candidates are schematically shown in Fig. 4.

A rectification scheme is required before the blast enters the cellular medium. The preferred approach is depicted in Fig. 3. A buffer plate, with a mass/area, m_p, is positioned to face the blast and the compressible material is mechanically attached. The buffer acquires a momentum per area, M, equal to the transmitted impulse per unit area, I_{trans}. Because the impulse remains unchanged as it transmits, to reduce the pressure to p_{th}, the medium extends the pulse duration [33]. Note that, the larger the m_p, the lower both the kinetic energy (KE) acquired by the buffer ($KE = M^2/2m_p$) and its velocity, $v = M/m_p$. If the kinetic energy transmitted into the protected structure (behind the cellular system) is small, most of the buffer plate kinetic energy is absorbed by inelastic dissipation mechanisms occurring within a densification front that passes through the medium, starting at the buffer. For a material with "ideal" mechanical response, Fig. 3(b), characterized by a constant unidirectional crushing stress, σ_{pl}, the maximum dissipation per area is, $U = \sigma_{pl}\varepsilon_D h$, where h is the thickness that crushes and $\varepsilon_D = 1 - \overline{\rho}$ is the strain at densification with $\overline{\rho}$ being the cellular material's relative density.

Equating the dissipation and kinetic energies gives the minimum cellular material thickness needed to arrest the buffer plate:

$$h_{min} = \frac{M^2}{2m_p\sigma_{pl}(1-\overline{\rho})} \tag{2}$$

Provided that the actual thickness exceeds h_{min}, the transmitted pressure will not exceed σ_{pl}. When thinner, densification occurs and much larger pressures are transmitted. The total mass per area to mitigate the pressure is:

$$m_{total} = h_b\rho_b + h_{min}\rho_s\overline{\rho} = h_b\rho_b + \frac{M^2}{2\sigma_{pl}(1-\overline{\rho})h_b\rho_b}\rho_s\overline{\rho} \tag{3}$$

where h_b is the buffer plate thickness, ρ_b its density and ρ_s is the density of the material used to make the cellular medium. This analysis leads to a minimum mass per area:

$$m_{total}^{min} = M\sqrt{\frac{2\overline{\rho}\rho_s}{\sigma_{pl}\varepsilon_D}} \tag{4}$$

If $\sigma_{pl} = p_{th}$ is specified as the constraint, then for a given impulse, the density terms are the only parameters affecting the minimum mass.

The preceding formulae are used to construct mitigation curves for a fixed explosive mass (10 kg of TNT) using an Al alloy foam with 5% relative density that compresses at 0.28 MPa (just below the injury threshold of 0.3 MPa) [19]. Using impulses ascertained from Fig. 2, the minimum foam thickness has been calculated as a function of stand-off distance for buffers with a mass per area of 8, 20 and 40 kg/m^2 (corresponding to 1, 2.5 and 5 mm of steel, respectively) as plotted in Fig. 5. Note that to mitigate a 1 kPa s impulse, corresponding to a 3 m standoff (Fig. 2), by using a buffer with a mass of 20 kg/m^2, a minimum foam thickness, $h_{min} = 10$ cm is required. More intense impulses require yet more bulky systems.

To substantiate these analytic results, decoupled dynamic simulations of crushing have been performed using the same foam and various buffer plates. The calculations have been conducted using ABAQUS/Explicit. The foam is considered to be rate insensitive (typical for Al alloys) [19] and the impulse is imparted to the buffer as a pressure/time history of the type expressed by Eq. (1), with $t_i \approx 0.044$ ms and $p_0 \approx 2.5$ MPa, such that the impulse $I_{total} \approx 1.1$ kPa s. The simulations have been performed using a foam thickness $h = 10$ and 15 cm. The results (Fig. 6) reveal that, at $h = 15$ cm, the foam crushes with average transmitted stress remaining below the threshold pressure. Moreover, the buffer arrests before the foam attains its densification strain. However, there are superimposed oscillations, which attain stresses as high as 0.4 MPa, albeit for short times. It remains to be determined whether these oscillations are transmitted and could cause injury. At $h = h_{min} = 10$ cm, the foam completely crushes after about 3.4 ms and large stress oscillations develop when the moving buffer pushes into the crushed foam. This calculation affirms that problems arise if the foam thickness is insufficient and ascertains the magnitude of the transmitted overstress when this happens. *They also reveal that the analytic method somewhat underestimates the critical thickness, suggesting that numerical simulations are needed to refine the determination of* h_{min}.

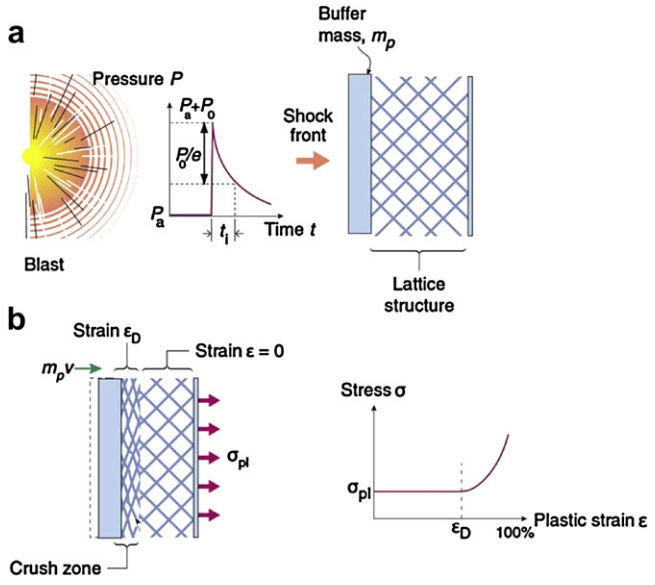

Fig. 3. A schematic of the passive blast mitigation system. In (a) the detonation creates a shock with a peak overpressure p_o and a decay time, t_i. The impulse, I_o, impinges onto a buffer, imparting momentum and causing it to accelerate to an initial velocity that varies inversely with its mass per unit area. In (b) the kinetic energy of the buffer is dissipated by the dissipation that occurs upon crushing of the cellular medium. The transmitted stresses are controlled by the flow strength of the cellular medium, which depends upon its topology, relative density and the material from which it is made.

4. The active concept

Analytic estimates. To explore active mitigation, we note that a shock propagating from a 10 kg TNT charge to an object placed 3 m away arrives in $t_{arrive} \approx 2$ ms, Fig. 2(c). [At 6 m, the time increases to $t_{arrive} \approx 7$ ms.] A sensor capable of detecting the electromagnetic emission [34–37] created at the instant of detonation would thus afford a time delay, t_{arrive}, between detonation and the arrival of the blast wave. This delay provides an opportunity to deploy a buffer by using a high-speed actuator, such as a propellant, Fig. 7. The force exerted on the buffer as it deploys must assure that the reaction pressure exerted on the protected structure does not exceed p_{th}. *The caveat is that reflection of the actuation pressure at the biological surface must not amplify the pressure transmitted*

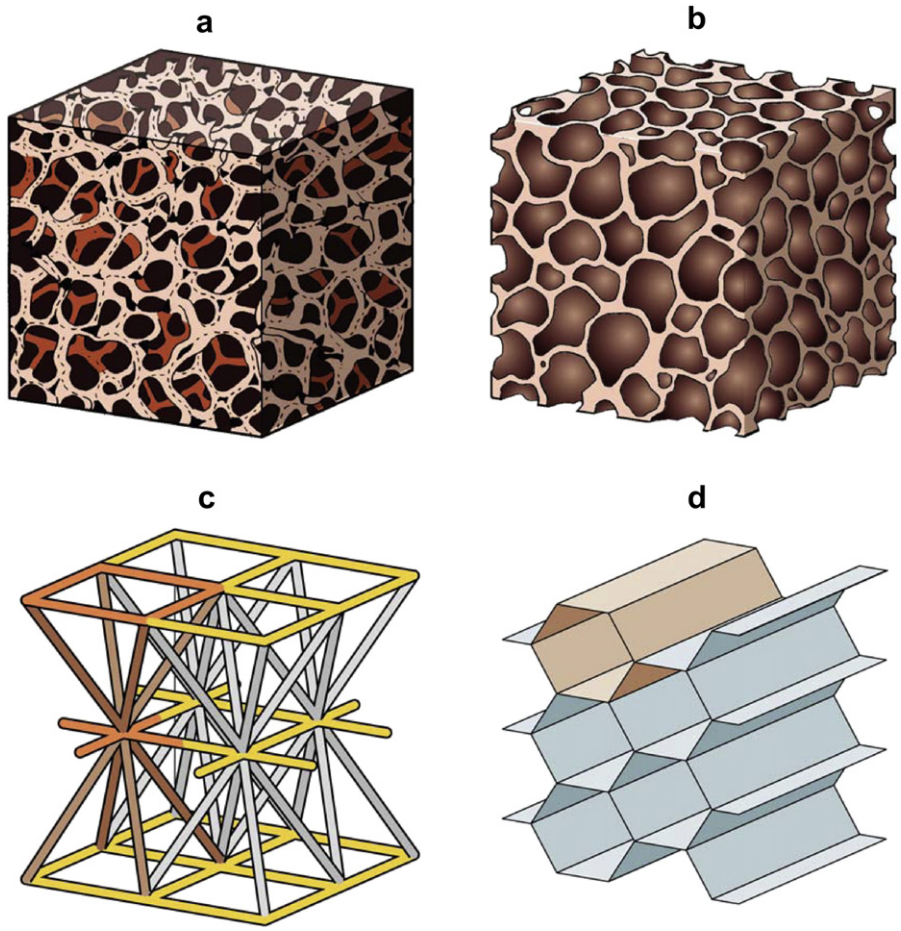

Fig. 4. Examples of cellular materials that could be used for blast mitigation. (a) An open cell foam. (b) A closed cell foam. (c) A multilayer lattice truss. (d) A prismatic corrugated core.

(backward) into the medium. This can be realized by the appropriate design of the pressure profile of the deployment system.

The maximum distance, x_{deploy}, moved by the buffer during t_{arrive} is:

$$x_{\text{deploy}} = p_{\text{th}} t_{\text{arrive}}^2 / 2m_{\text{p}}. \tag{5}$$

The momentum acquired by the buffer during deployment is:

$$M_{\text{cancel}} = -p_{\text{th}} t_{\text{arrive}} \tag{6}$$

At the instant it collides with the blast wave, the buffer has momentum:

$$M_{\text{buffer}} = M_{\text{blast}} + M_{\text{cancel}} \tag{7}$$

When $M_{\text{cancel}} > M_{\text{blast}}$, the buffer plate continues to move outward until it reaches its deployment limit. When $M_{\text{cancel}} < M_{\text{blast}}$, the buffer reverts to backward motion with velocity, $v_{\text{back}} = M_{\text{buffer}}/m_{\text{p}}$, at distance x_{deploy} from its original position. Since the cellular medium retains crushing strength, p_{th}, the velocity of the buffer when it returns to its position before deployment is:

$$v_{\text{final}} = (1/m_{\text{p}})\sqrt{M_{\text{buffer}}^2 - M_{\text{cancel}}^2} \tag{8}$$

By assuring that $M_{\text{buffer}}^2 > M_{\text{cancel}}^2$, the mitigation system defeats the blast. The criterion for success is thus:

$$M_{\text{blast}} + 2M_{\text{cancel}} \leq 0. \tag{9}$$

The implication is that, for the device shown in Fig. 7 with a buffer plate mass $m_{\text{p}} = 20\ \text{kg/m}^2$ subjected to a 10 kg explosion at a 3 m standoff, since $M_{\text{cancel}} \approx -0.6$ kPa s and $M_{\text{blast}} = 1.1$ kPa s, a compact system that retains its crushing strength after deployment just defeats the impulse.

Numerical simulations. To assess the conclusions of this simplified analysis, detailed numerical simulations of coupled fluid–structure interaction (FSI) in air have been conducted by considering the plate as rigid, but able to move as a result of the deployment and blast pressure exerted upon it. The significance of the fluid–structure interaction depends on the mass per unit area of the buffer plate (or front face of a sandwich panel). For practical plate thicknesses, the mass per unit area is sufficient that the fluid–structure interaction effect in air is minimal [25].

The piecewise parabolic method [38,39] for the one-dimensional (spherically-symmetric) Euler equation in Lagrangian form is used to solve for the flow field, i.e. density, velocity and pressure, in the fluid domain. The buffer plate is assumed to be perfectly rigid and its dynamics is governed by Newton's second law:

$$m_{\text{p}}\dot{v} = p - p_0 - p_{\text{th}} \tag{10}$$

$$\dot{x} = v \tag{11}$$

where m_{p} is the mass of the buffer plate ($20\ \text{kg/m}^2$), x the plate coordinate, v the plate velocity, p_0 the constant ambient static pressure on the right side of the plate, p_{th} (0.28 MPa) the deployment

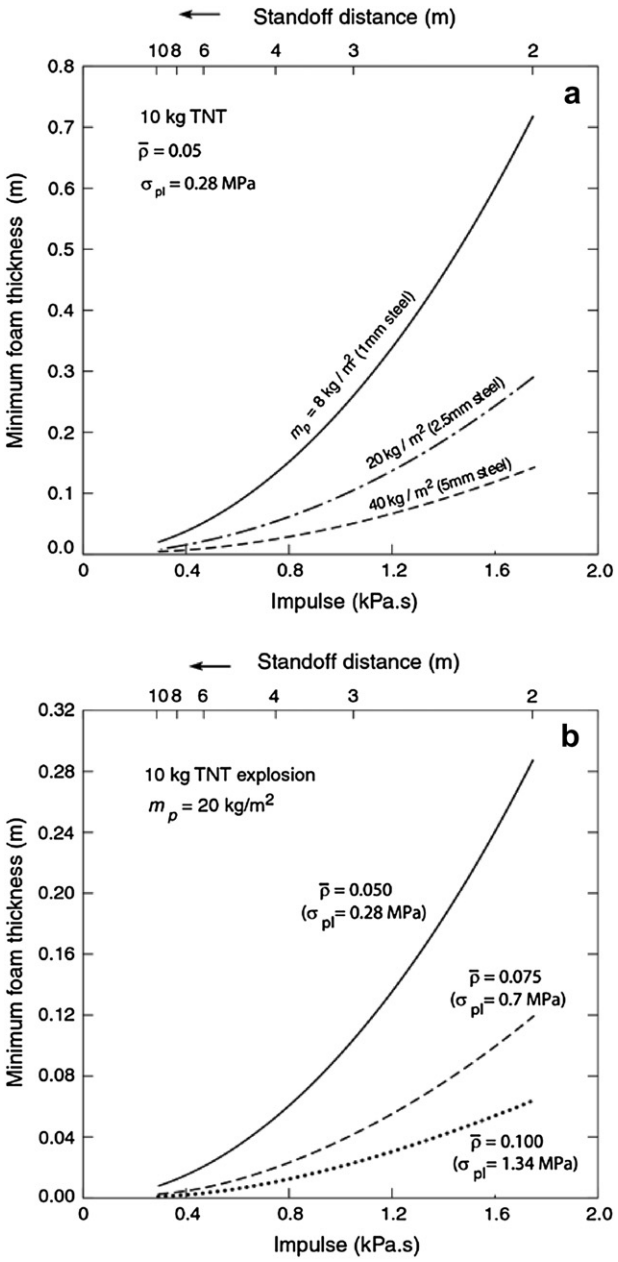

Fig. 5. (a) The minimum aluminum foam thickness required to arrest buffer plates of various masses per unit area (m_p) when the maximum transmitted stress is constrained to be no more than 0.28 MPa. The impulse applied to the buffer resulted from the explosion of 10 kg of TNT at various standoffs. Heavy buffers acquire a smaller initial velocity (and kinetic energy) and can be arrested with less foam. (b) The effect of foam strength (implicitly controlled by relative density) upon the minimum foam thickness required to arrest a buffer with a mass per area of 20 kg/m^2. Stronger foams would be thinner but transmit larger stresses.

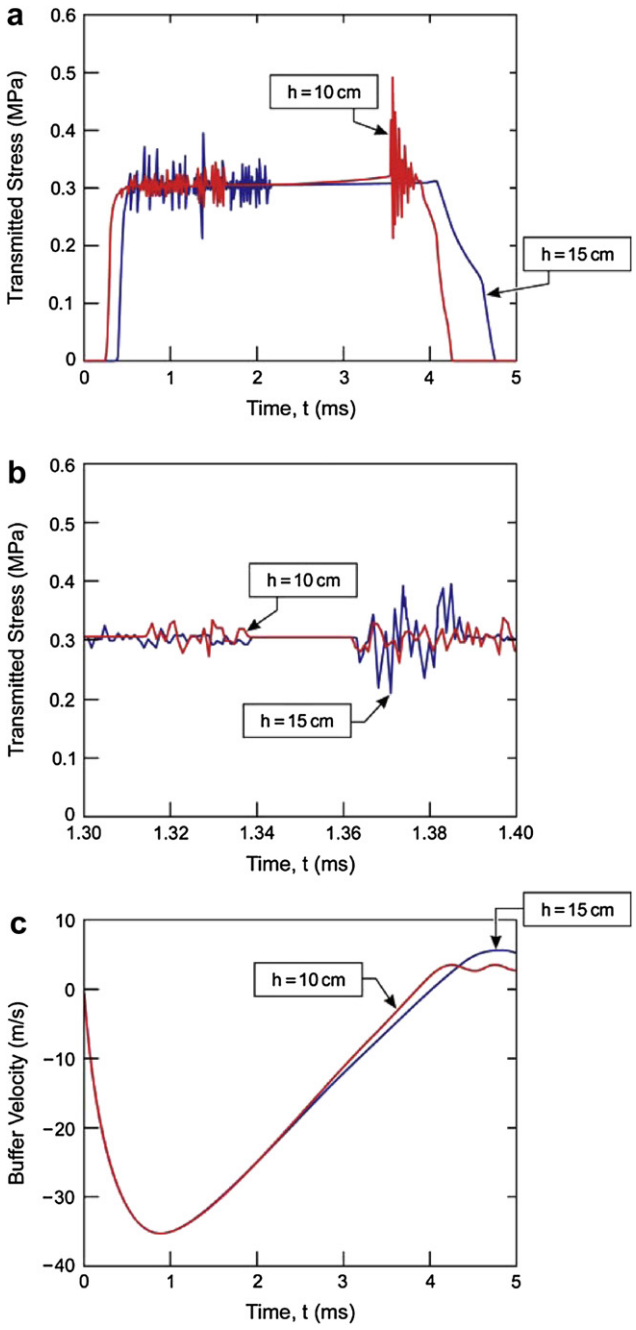

Fig. 6. Finite element simulations using an aluminum foam behind a buffer plate of mass, $m_p = 20$ kg/m^2 and impulse, 1.1 kPa s at two different thicknesses of foam. (a) The temporal dependence of the transmitted pressure. (b) An expanded view of the pressure oscillations between 1.3 and 1.4 ms. (c) The velocity of the buffer plate and its eventual arrest.

pressure, and p the fluid pressure acting on the plate. The initial conditions adopted for the blast flow field correspond to the spherical point source solution of Okhotsimskii et al. [40]. A schematic of the simulation setup is shown in Fig. 8. The center of explosion is at $x = -3.0$ m and the buffer plate is at $x = 0.0$ m at time $t = 0.0$ ms.

Outflow boundary conditions are applied on the left of the computational fluid domain, whereas a constant pressure ($p_{th} + p_0$) is applied on the right to simulate the deployment conditions. Fig. 8 shows the pressure distribution and the build up of the compression wave ahead of the deploying plate at $t = 1.25$ ms. Eq. (10) governing the plate dynamics is integrated in time using the Crank–Nicholson scheme, and the coupled interaction between the plate and the fluid is accomplished using a partitioned scheme [41].

The temporal evolution of the position and velocity of the buffer, as well as the pressure history on its face, are plotted in Fig. 9 for three explosive charges (10, 12.5, 15 kg of TNT) located at a 3 m standoff. The ambient pressure is assumed to be 1 atm (0.1 MPa). In the figure, a positive (negative) ordinate position implies that the buffer has moved away from (towards) the blast. Under the action of a constant deployment pressure of $p_{th} = 0.28$ MPa, it initially moves towards the incoming blast, with an ostensibly constant

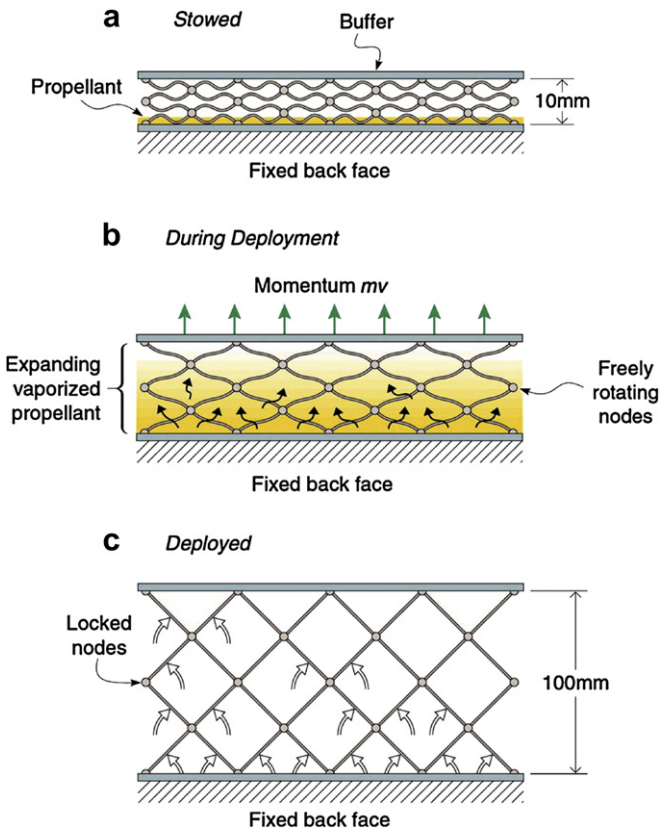

Fig. 7. An example of a deployment scheme for an active mitigation concept.

acceleration, affected only by the opposing air pressure exerted on the front. The impact of the blast causes the buffer to decelerate and in some cases, invert its direction of motion. The rapidly decaying blast overpressure is supplanted by the continued application of the deployment pressure, which eventually causes the buffer to arrest at a maximum penetration into the medium. This circumstance coincides with the criterion for vanishing final velocity used in the simplified analysis. Note, however, that, unlike the simple

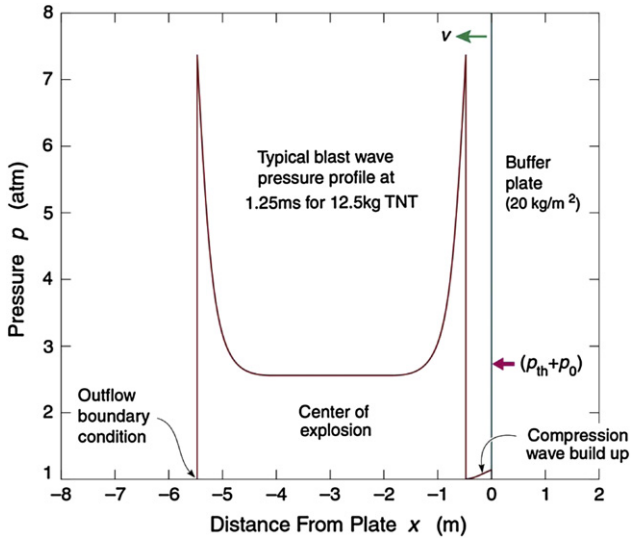

Fig. 8. Schematic of the simulation setup showing the blast wave pressure at $t = 1.25$ ms and the build up of the compression wave ahead of the buffer, due to its motion.

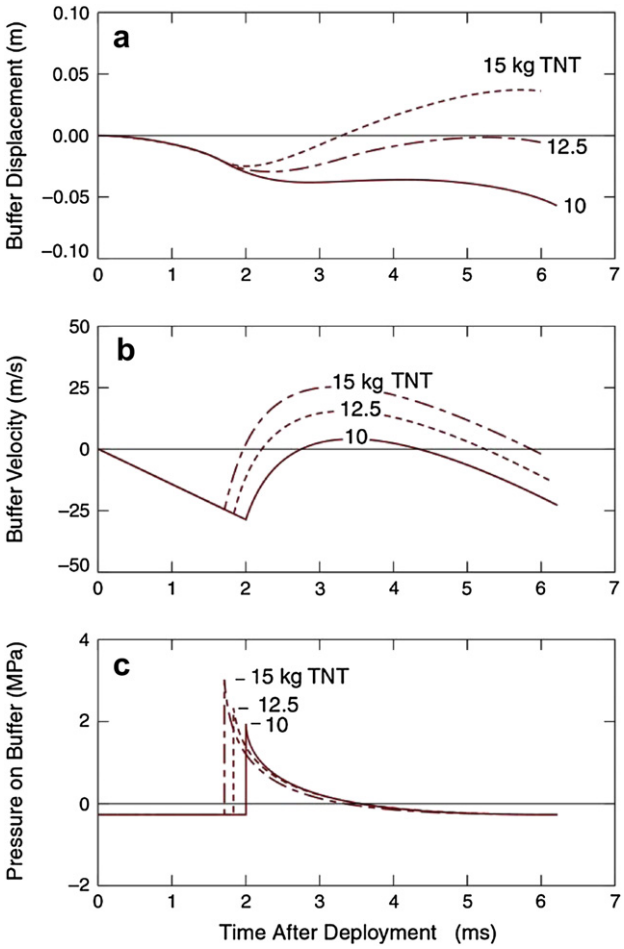

Fig. 9. Results from the simulations. (a) The temporal variation in the displacement of the buffer for three different levels of explosion intensity (10, 12.5 and 15 kg TNT). Note that the buffer moves beyond its original location for the largest explosive mass and, thus, crashes into the structure to be protected: whereas it remains beyond this location for the two smaller explosions. (b) The corresponding velocities indicate that the time at zero velocity does not coincide with that at maximum penetration. (c) The temporal dependence of the total pressure on the buffer.

analysis which required a zero (or negative) final velocity, this criterion does not assure that the buffer arrests at its initial location, as evident from the result for 15 kg of TNT. Nevertheless, the simple analysis, based on ConWep generated information, is conservative. Namely, at the analytically predicted threshold of 10 kg of TNT, the buffer arrests beyond its original location. The actual defeat threshold is attained for a charge of 12.5 kg. This discrepancy highlights the importance of using a computational capability that incorporates the coupled FSI effects. These approaches reveal how the blast intensity determines the maximum displacement of the buffer toward the blast, the time of impact, the rate at which the blast reverses the motion and, most importantly, the maximum penetration of the buffer into the expanded cellular medium.

5. Summary

Explosions in air can cause damage in at least six different ways: (i) by their reaction to the impulse associated with the primary blast wave, (ii) by secondary fragment impact, (iii) by burning upon contact with high temperature gases created during the detonation, (iv) by acceleration into a rigid object, (v) by differential momentum transfer to appendages, and (vi) by the collapse of

surrounding structures. The present article addressed the first of these by devising concepts for the prevention of damage caused by the primary blast wave.

In the passive approach, highly compressible cellular media designed to collapse at a constant pressure, just below the user chosen threshold (e.g. that which causes damage to biological tissues), enable blast mitigation when rectified with an attached buffer of appropriate mass. However, at representative levels of blast, these passive systems are shown to be excessively bulky. A reactive concept based upon the deployment of an inflatable cellular structure facilitates momentum cancellation and is shown to achieve mitigation with substantially more compact (and lighter) solutions.

Acknowledgements

The active mitigation concepts discussed in this paper were initially developed during a study conducted by the Defense Science Research Council and we are grateful to Geoffrey Ling, Brett Giroir, Rick Satava and Judith Swain for stimulating discussions of this topic. We are grateful to the Defense Advanced Research Projects Agency for its support of the Council and to the Office of Naval Research for its support of the subsequent analysis of reactive cellular material mitigation concepts under grant number N00014-01-1-1051 monitored by Dr. David Shifler.

References

[1] Baker WE. Explosions in air. Austin, TX: University of Texas Press; 1973.
[2] Smith PD, Hetherington JG. Blast and ballistic loading of structures. Butterworth-Heinemann; 1994.
[3] Swisdak Jr MM. Explosion effects and properties: part i – explosion effects in air. Silver Spring, MD: NSWC/WOL/TR 75-116 White Oak; 1975.
[4] Fundamentals of protective design for conventional weapons, TM 5-855-1. Washington, DC: Department of the Army; 1986.
[5] Dharmasena KP, Wadley HNG, Xue Z, Hutchinson JW. Mechanical response of metallic honeycomb sandwich panel structures to high intensity dynamic loading. International Journal of Impact Engineering 2008;35:1063–74.
[6] ConWep Blast simulation Software. U.S. Army Corps Engineers, Vicksburg, MS.
[7] Wightman JM, Gladish SL. Explosions and blast injuries. Annals of Emergency Medicine 2001;37(6):664–78.
[8] Horrocks C, Brett S. Blast injury. Current Anesthesia and Critical Care 2000;11:113–9.
[9] Roberts P. Patterns of injury in military operations. Current Anesthesia and Critical Care 2003;13:243–8.
[10] Cooper GJ, Maynard RL, Cross NL, Hill JF. Casualties from terrorist bombings. The Journal of Trauma 1983;23:955–67.
[11] Taber KH, Warden DL, Hurley RA. Blast-related traumatic brain injury: what is known? Journal of Neuropsychiatry and Clinical Neuroscience 2006;18(2):141–5.
[12] Cooper GJ. Protection of the lung from blast overpressure by thoracic stress wave decouplers. The Journal of Trauma 1996;40:S105–10.
[13] Stuhmiller JH. Biological response to blast overpressure: a summary of modeling. Toxicology 1997;121:91–103.
[14] Stuhmiller JH, Ho KHH, Vander Vorst MJ, Dodd KT, Fitzpatrick T, Mayorga M. A model of blast overpressure injury to the lung. Journal of Biomechanics 1996;29:227–34.
[15] Bowen IG, Fletcher ER, Richmond DR, Hirsch FG, White CS. Biophysical mechanisms and scaling procedures applicable in assessing responses of the thorax energized by air-blast overpressure or by nonpenetrating missiles. Annals of New York Academy of Sciences 1968;152:122–46.
[16] Elsayed N. Toxicology of blast overpressure. Toxicology 1997;121:1–15.
[17] Bass CR. private communication; 2006.
[18] Langdon GS, Nurick GN, Balden VH, Timmis RB. Perforated plates as passive mitigation systems. Defence Science Journal 2008;58(2):238–47.
[19] Ashby MF, Evans AG, Fleck NA, Gibson LJ, Hutchinson JW, Wadley HNG. Metal foams: a design guide. London: Butterworth-Heinemann; 2000.
[20] Gibson LJ, Ashby MF. In: Cellular solids: structure and properties. 2nd ed. Cambridge University Press; 1997.
[21] Leishman JG. Principles of helicopter aerodynamics. Cambridge University Press; 2006.
[22] Kim DH, Park JW, Lee GS, Lee KI. Active impact control system design with a hydraulic damper. Journal of Sound and Vibration 2002;250(3):485–501.
[23] Gavrila DM. Sensor-based pedestrian protection. IEEE Intelligent Systems 2001;16(6):77–81.
[24] Tilp J, et al. Pedestrian protection based on combined sensor systems. In: Tenth international technical conference on the enhanced safety of vehicles, Washington, DC; 2005.
[25] Kambouchev N, Noels L, Radovitzky R. Fluid–structure interaction effects in the loading of free-standing plates by uniform shocks. Journal of Applied Mechanics 2007;74.
[26] Kambouchev N, Noels L, Radovitzky R. Compressibility effects on fluid-structure interaction and their implications of the air blast loading of structures. Journal of Applied Physics 2006;100.
[27] Vaziri A, Hutchinson JW. Metal sandwich plates subject to intense air shocks. International Journal of Solids & Structures 2007;44:2021–35.
[28] Kambouchev N, Noels L, Radovitzky R. Numerical simulation of the fluid–structure interaction between air blast waves and free-standing plates. Computers and Structures June 2007;85:923–31.
[29] Noels L, Dharmasena K, Wadley H, Radovitzky R. Air shock loading of metallic plates: experiments and coupled simulations. International Journal of Impact Engineering, submitted for publication.
[30] Avasarala SR, Bui-Tanh T, Wadley H, Radovitzky R. Blast mitigation using air-depleted sandwich panels, in preparation.
[31] Bitzer T. Honeycomb technology. Chapman and Hall; 1997.
[32] Wadley HNG, Dharmasena KP, Chen Y, Dudt P, Knight D, Kiddy K. Compressive response of multilayered pyramidal lattices during underwater shock loading. International Journal of Impact Engineering 2008;35:1102–14.
[33] Dharmasena KP, Queheillalt DT, Wadley HNG, Dudt P, Chen Y, Knight D, et al. Dynamic compression of metallic sandwich structures during planar impulsive loading in water. European Journal of Mechanics – A/Solids 2010;29:56–67.
[34] Anderson WH, Long CL. Electromagnetic radiation from detonating solid explosives. Journal of Applied Physics 1965;36(4):1494–5.
[35] van Lint VAJ. Electromagnetic emission from chemical explosions. IEEE Transactions on Nuclear Science 1982;NS-29(6).
[36] Fine JE, Vinci SJ. Causes of electromagnetic radiation from detonation of conventional explosives: a literature survey. Army Research Laboratory Report, ARL-TR-1690; 1998. p. 19–23.
[37] Orson JA, Bagby WF, Perram GP. Infrared signatures from bomb detonations. Infrared Physics & Technology 2003;44:101–7.
[38] Colella P, Woodward PR. The piecewise parabolic method (PPM) for gas dynamical simulations. Journal of Computational Physics 1984;54:174–201.
[39] Stone J. The CMHOG code. Available from: <http://www.astro.princeton.edu/jstone/cmhog.html>.
[40] Okhotsimskii DE, Kondrasheva IA, Vlasova ZP, Kozakova RK. Calculation of a point explosion taking into account counter pressure. Tr Mat Inst Steklova 1957;50:1–65.
[41] Felippa CA, Park KC, Farhat C. Partitioned analysis of coupled mechanical systems. Computer Methods in Applied Mechanics and Engineering 2001;190:3247–70.